ACS Macro Letters

Letter

Cite This: ACS Macro Lett. 2018, 7, 281−286

pubs.acs.org/macroletters

Synthesis and Direct Observation of Thermoresponsive DNA Copolymers

Songsong Li[†] and Charles M. Schroeder*[,†,‡]

[†]Department of Materials Science and Engineering, University of Illinois at Urbana—Champaign, Urbana, Illinois 61801, United States

[‡]Department of Chemical and Biomolecular Engineering, University of Illinois at Urbana—Champaign, Urbana, Illinois 61801, United States

Supporting Information

ABSTRACT: Single-molecule techniques allow for the direct observation of long-chain macromolecules, and these methods can provide a molecular understanding of chemically heterogeneous and stimuli-response polymers. In this work, we report the synthesis and direct observation of thermoresponsive DNA copolymers using single-molecule techniques. DNA-PNIPAM copolymers are synthesized using a two-step strategy based on polymerase chain reaction (PCR) for generating linear DNA backbones containing non-natural nucleotides (dibenzocyclooctyne-dUTP), followed by grafting thermoresponsive side branches (poly(*N*-isopropylacrylamide), PNIPAM) onto DNA backbones using copper-free click chemistry. Single-molecule fluorescence microscopy is used to directly observe the stretching and relaxation dynamics of DNA-PNIPAM copolymers both below and above the lower critical solution temperature (LCST) of PNIPAM. Our results show that the intramolecular conformational dynamics of DNA-PNIPAM copolymers are affected by temperature, branch density, and branch molecular weight. Single-molecule experiments reveal an underlying molecular heterogeneity associated with polymer stretching and relaxation behavior, which arises in part due to heterogeneous chemical identity on DNA copolymer dynamics.

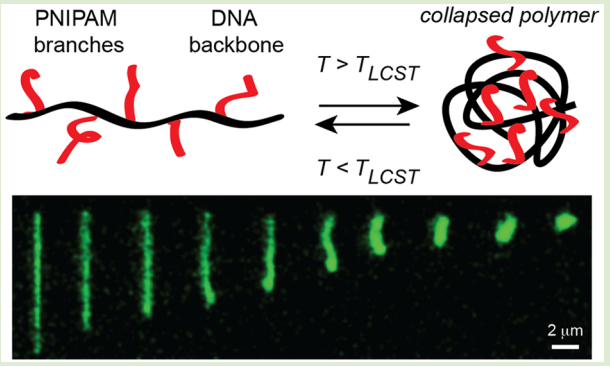

The chemical composition of long-chain macromolecules plays a key role in determining the emergent physical and structural properties of polymeric systems.[1] Copolymers and block polymers with simple linear chain architectures can give rise to intricate structural ordering and assembly across multiple length scales.[2,3] In addition to chemical identity, polymer chain architecture also plays a key role in supramolecular assembly, with chain topologies and shapes including linear, branched, ring, and cross-linked polymers.[4] Synthetic strategies for controlling polymer composition and architecture have been used to develop materials for applications including encapsulation for drug delivery,[5] gene delivery,[6] catalysis,[7] and surfactants for emulsion stabilization.[8]

In recent years, biohybrid materials containing both synthetic and natural components have been developed, which has provided intriguing new materials with increased biocompatibility, controlled biodegradation, broad chemical functionality, and unprecedented levels of sequence control.[9−12] In particular, DNA copolymers[13−17] have been shown to self-assemble into various supramolecular architectures such as micelles,[17] vesicles,[18] and tubular structures.[19] Despite recent work, however, we still lack a full understanding of the effects of chemistry, architecture, and hydrophilicity/hydrophobicity on the conformational dynamics of DNA-based copolymers.

Single-molecule techniques offer an ideal strategy to directly study the conformational dynamics of macromolecules.[20−22] In recent years, DNA has served as a model polymer for fundamental studies of nonequilibrium polymer dynamics ranging from dilute to entangled polymer solutions.[23−28] However, the vast majority of prior single polymer studies has largely focused on dynamic studies of chemically homogeneous, linear DNA. Recent work has extended the field of single polymer dynamics to chains with nonlinear architectures including ring polymers and comb polymers,[21,25,26,29] though these macromolecules generally consist of natural DNA. On the other hand, molecular assembly of DNA-based materials has been studied using bulk spectroscopic methods.[16] However, the conformational dynamics of chemically heterogeneous copolymers has not yet been fully explored at the single-molecule level. From this view, development of new methods to directly image the triggered response or assembly of functional copolymers at the single-molecule level would provide new insights into the molecular-scale dynamics of these materials. For example, direct imaging of the thermally

Received: January 5, 2018
Accepted: February 11, 2018

DOI: 10.1021/acsmacrolett.8b00016
ACS Macro Lett. 2018, 7, 281−286

Scheme 1. Synthesis of DNA-PNIPAM Copolymers

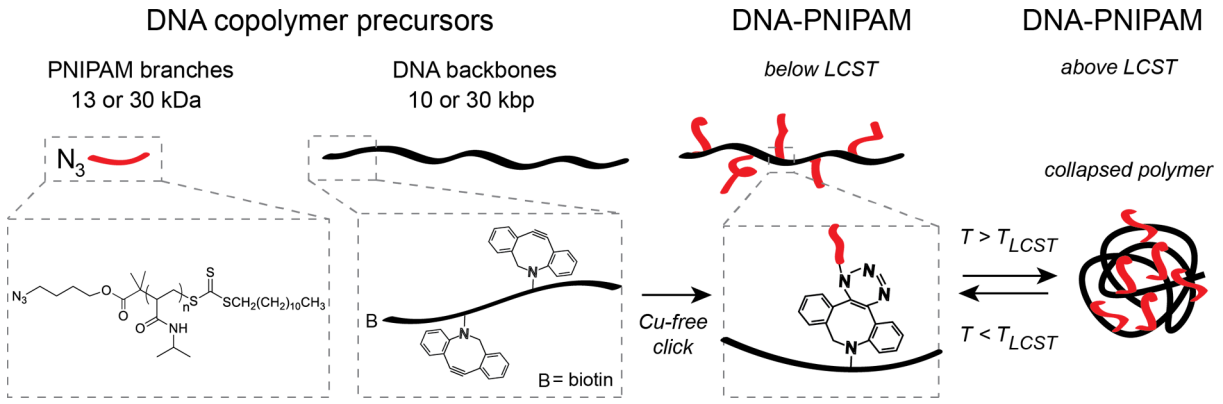

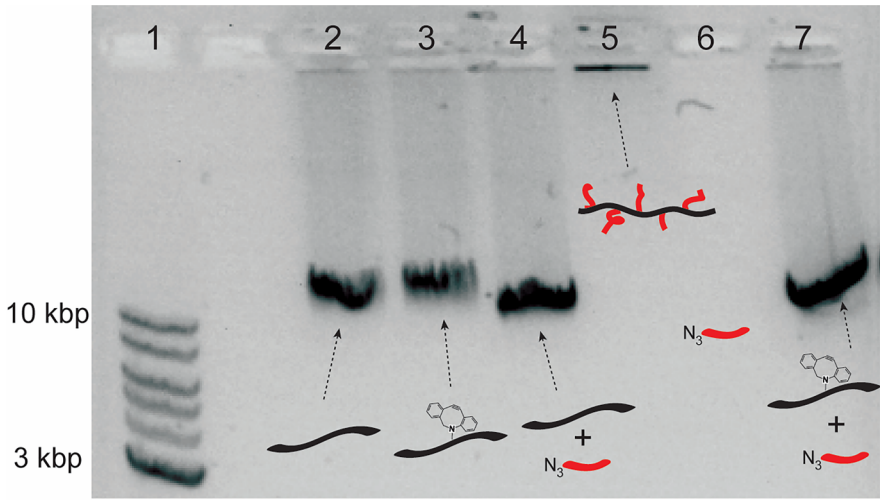

Figure 1. Agarose gel electrophoresis of DNA-PNIPAM copolymers and precursors. Lane 1: 1 kbp DNA ladder. Lane 2: 10 kbp natural DNA. Lane 3: 10 kbp DBCO-DNA with 1% DBCO substitution. Lane 4: 10 kbp natural DNA with 13 kDa PNIPAM-azide. Lane 5: 10 kbp DBCO-DNA with 13 kDa PNIPAM-azide (after reaction). Lane 6: 13 kDa PNIPAM-azide. Lane 7: 10 kbp DBCO-DNA with 13 kDa PNIPAM-azide (before reaction). Samples are stained with SYBR Gold and electrophoresed in 0.6% agarose in 1X TAE buffer at 120 V for 30 min.

activated response of DNA-PNIPAM copolymers at the single-chain level could reveal molecular distributions and unexpected heterogeneous behavior, thereby providing new information beyond traditional bulk cloud point measurements.

In this work, we report the synthesis and direct observation of thermoresponsive DNA copolymers consisting of a main chain DNA backbone with grafted poly(*N*-isopropylacrylamide) (PNIPAM) side branches. PNIPAM is a thermoresponsive polymer exhibiting a reversible hydrophilic to hydrophobic transition when the temperature is raised above the lower critical solution temperature (LCST) (32 °C).[30,31] From this perspective, PNIPAM is a suitable material to generate DNA copolymers with temperature-sensitive properties near or slightly above room temperature. Following synthesis and characterization, single-molecule fluorescence microscopy is used to observe the conformational stretching and relaxation dynamics of single DNA-PNIPAM copolymers both below and above the LCST of PNIPAM. Our results show that the hydrophilic−hydrophobic transition for PNIPAM side branches results in enhanced intramolecular interactions, leading to dynamic heterogeneity in single polymer behavior. In particular, experiments reveal broadly distributed probabilities of polymer chain extension above the LCST and altered conformational relaxation dynamics due to PNIPAM side branches. Taken together, these results demonstrate the utility of studying the dynamics of biohybrid copolymers using single-molecule imaging.

We began by synthesizing thermoresponsive DNA copolymers via strain-promoted [3 + 2] alkyne−azide cycloaddition (SPAAC) (Scheme 1). Azide-terminated PNIPAM was synthesized by reversible addition−fragmentation chain transfer (RAFT) polymerization using a chain transfer agent (CTA) containing a terminal azide group (Supporting Information). Using this approach, two samples of azide-terminated PNIPAM were synthesized with different molecular weights (M_n = 13 kDa (PDI = 1.03) and 30 kDa (PDI = 1.01), characterized by gel permeation chromatography). In a separate reaction, DNA molecules containing non-natural nucleotides (dibenzocyclooctyne-dUTP, DBCO-dUTP) were synthesized using polymerase chain reaction (PCR), which allows for the preparation of perfectly monodisperse DNA backbones (10 or 30 kbp). During PCR, DBCO loading was controlled by varying the ratio of natural dTTP to non-natural DBCO-dUTP in the reaction mixture (Tables S1 and S2). Moreover, a single biotin group was included at one DNA terminus using a chemically modified PCR primer, which allows for surface tethering of DNA-PNIPAM copolymers via biotin−streptavidin interactions for single-molecule imaging.

DOI: 10.1021/acsmacrolett.8b00016
ACS Macro Lett. 2018, 7, 281−286

Following PCR, azide-terminated PNIPAM branches were covalently linked to DNA backbones using a graft-onto reaction via SPAAC (Supporting Information). Branch density is controlled by varying the amount of DBCO incorporation in DNA backbones, with a 1% incorporation of DBCO-dUTP (1% dTTP replaced with DBCO-dUTP) yielding a relatively low branch loading (one branch per 400 base pairs) and a 10% incorporation of DBCO-dUTP yielding a higher branch loading (one branch per 40 base pairs). Following the copper-free click reaction, DNA-PNIPAM copolymers were purified using a microspin centrifuge column (100 kDa MWCO) and characterized using agarose gel electrophoresis (Figures 1 and S1). In all cases, the electrophoretic mobility of 10 kbp natural DNA is similar to DBCO-DNA (with 1% and 10% of dTTP replaced with DBCO-dUTP). However, branched DNA-PNIPAM copolymers show a substantial decrease in electrophoretic mobility. These results are consistent with prior work showing reduced electrophoretic mobility for chemically homogeneous branched DNA such as comb-shaped or star-shaped DNA in agarose gel networks.[32]

Following synthesis, we studied the self-assembly behavior of DNA-PNIPAM copolymers as a function of temperature. DNA-PNIPAM copolymers were exchanged into an aqueous buffer (10 mM Tris/Tris-HCl, pH 8.0, 1 mM EDTA, and 300 mM NaCl), and the LCST of DNA-PNIPAM was found to be 30 °C (Figure S2), which is consistent with prior work.[30] Reaction products were then dried onto solid surfaces at 45 °C, significantly above the LCST of PNIPAM, followed by characterization using scanning electron microscopy (SEM) (Figure 2). Interestingly, SEM images show self-assembled structures for DNA-PNIPAM copolymers on the order of a few microns (Figure 2d) which agrees with dynamic light-scattering (DLS) experiments (Figure S2), whereas SEM images for control samples of DBCO-DNA and PNIPAM-azide showed much smaller structures on the order of 200 and 50 nm, as shown in Figures 2a and 2b, respectively. In addition, SEM images of 10 kbp natural DNA mixed with PNIPAM-azide (Figure 2c) appear similar to SEM images of 10 kbp DNA.[33] These results suggest that copolymer assembly only occurs when DNA-PNIPAM is treated above the LCST but not in the cases of DBCO-DNA or natural DNA mixed with PNIPAM-azide.

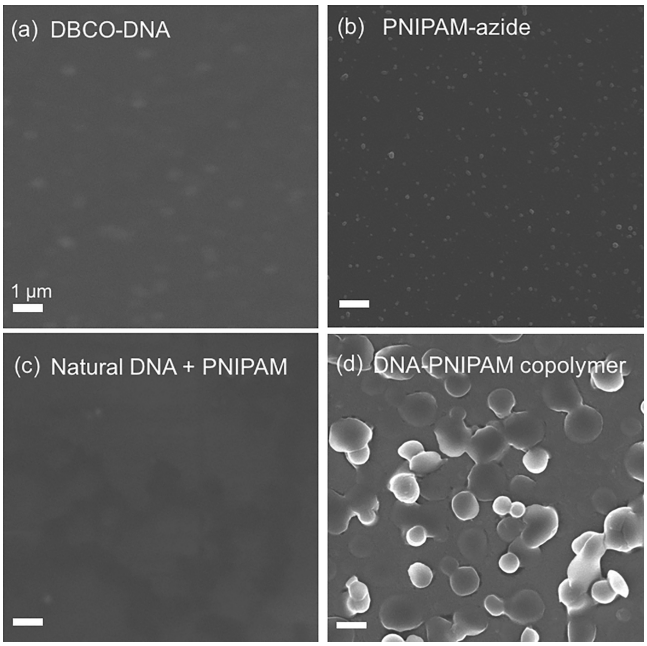

Figure 2. Representative SEM images of DNA-PNIPAM copolymers and precursors following drying at 45 °C. (a) DBCO-DNA (10 kbp), (b) PNIPAM-azide (13 kDa), (c) natural DNA (10 kbp) with PNIPAM-azide (13 kDa), and (d) DNA-PNIPAM copolymers (10 kbp backbone with 1% DBCO substitution, 13 kDa PNIPAM branches).

We next used single-molecule fluorescence microscopy to study the effects of temperature, PNIPAM branch density, and branch molecular weight on the stretching and relaxation dynamics of thermoresponsive DNA copolymers (Figure 3). In these experiments, DNA-PNIPAM copolymers are immobilized on a PEG/PEG-biotin glass coverslip surface in a microfluidic flow cell via specific biotin−NeutrAvidin interactions[34] (Figure 3a), thereby generating a field of end-tethered DNA-PNIPAM copolymers on a passivated surface. Surface-tethered polymer chains are stretched to high degrees of extension in a simple shear flow using pressure-driven flow, achieving a fractional chain extension $x/L \approx 0.75$ at high flow strengths ($W_i \approx 100$), where W_i is a dimensionless flow strength known as the Weissenberg number.[35] For polymer stretching experiments in this work, Weissenberg number is defined as $W_i = \tau\dot{\gamma}$, where τ is the longest relaxation time of the natural DNA polymer backbone and $\dot{\gamma}$ is the shear rate. DNA copolymer stretching experiments are performed in an aqueous buffer (10 mM Tris/Tris-HCl, pH 8.0, 1 mM EDTA, and 5 mM NaCl) containing an intercalating dye (SYTOX Green), which enables direct imaging of DNA backbones using fluorescence microscopy (Supporting Information).

Using this approach, we studied the effect of temperature on the stretched length distribution of 10 kbp DNA-PNIPAM copolymers (13 kDa PNIPAM) with 1% DBCO substitution (low branch loading) (Figure 3b and 3c). In this experiment, shear flow was used to stretch surface-tethered DNA-PNIPAM copolymers at 25 °C (corresponding to $W_i \approx 100$ for the natural DNA backbone), followed by heating the microfluidic device from 25 to 40 °C under no flow conditions. Next, the stretched length distribution of DNA-PNIPAM copolymers was again determined in the presence of shear flow at a temperature (40 °C) above the LCST of PNIPAM. Finally, the microfluidic device was cooled to 25 °C in the absence of flow, and the stretched length distribution was again observed at 25 °C. For each case, stretched length distributions are obtained over at least 100 molecules.

Single-molecule images of 10 kbp natural DNA and 10 kbp DNA-PNIPAM (13 kDa PNIPAM branches) copolymers at 25 and 40 °C are shown in Figure 3b. Image analysis is used to measure the stretched lengths of DNA and DNA-PNIPAM copolymers in flow, and the stretched length distributions are shown in Figure 3c and Table S3. Here, the theoretical contour length for fluorescently labeled 10 kbp DNA is 4.3 μm. Initially, the average stretched extension of 10 kbp DNA-PNIPAM is 3.0 ± 0.6 μm at 25 °C. Upon heating the sample to 40 °C, DNA-PNIPAM copolymers collapse and show much smaller stretched lengths in shear flow with an average size of 2.1 ± 0.7 μm. Finally, upon cooling the microfluidic device to 25 °C, the DNA-PNIPAM copolymers return to an extended conformation in flow with an average polymer extension of 3.1 ± 0.6 μm. On the other hand, 10 kbp natural DNA exhibits no appreciable changes in average stretched length with temperature, with an average extension of 3.3 ± 0.2 μm during

DOI: 10.1021/acsmacrolett.8b00016
ACS Macro Lett. 2018, 7, 281−286

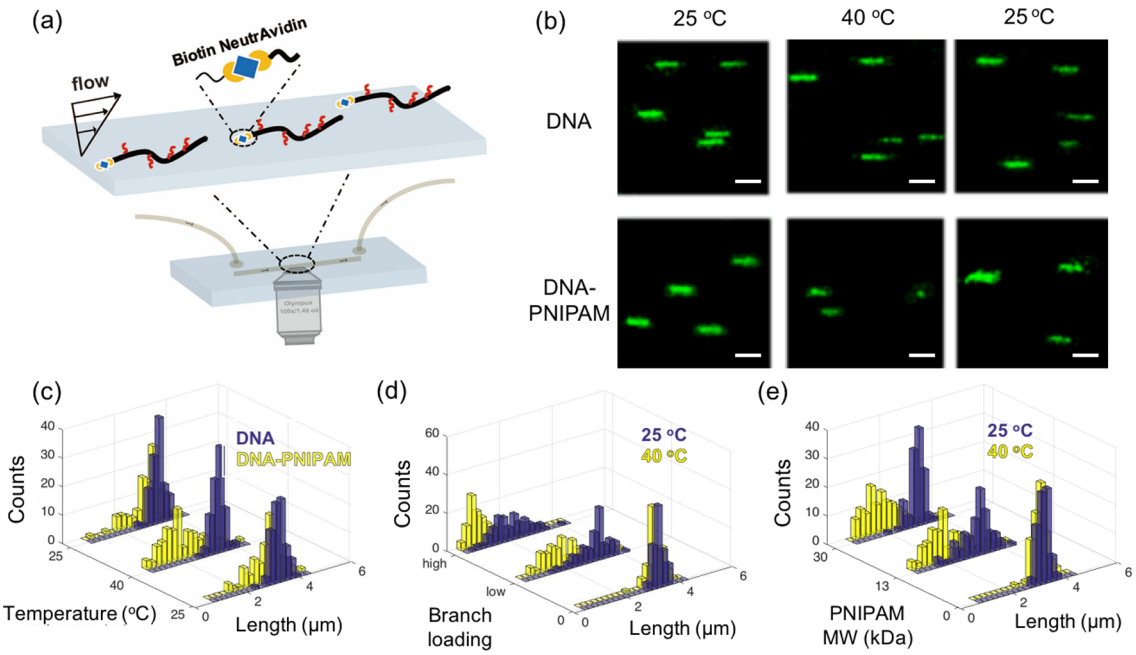

Figure 3. Single-molecule imaging of surface-tethered DNA-PNIPAM copolymers stretched in shear flow. (a) Schematic of experimental setup showing microfluidic flow cell and surface-tethered DNA-PNIPAM copolymers. (b) Series of single-molecule images of surface-tethered DNA-PNIPAM copolymers (10 kbp DNA backbones, 1% DBCO, 13 kDa PNIPAM branches) and DNA polymers (10 kbp DNA backbones) stretched in shear flow. DNA backbones are labeled with SYTOX Green. Scale bar: 5 μm. (c)−(e) Histograms showing probability of DNA backbone extension for tethered chains stretched in shear flow (minimum of N = 100 molecules in each histogram), showing (c) the effect of temperature, (d) branch density, and (e) PNIPAM branch molecular weight. Experiments in (c) and (e) are performed with low PNIPAM branching (10 kbp DNA backbones, 1% DBCO), whereas experiments in (d) are performed with low PNIPAM branching (10 kbp DNA, 1% DBCO, 13 kDa PNIPAM branches) and high branching (10 kbp DNA, 10% DBCO, 13 kDa PNIPAM branches).

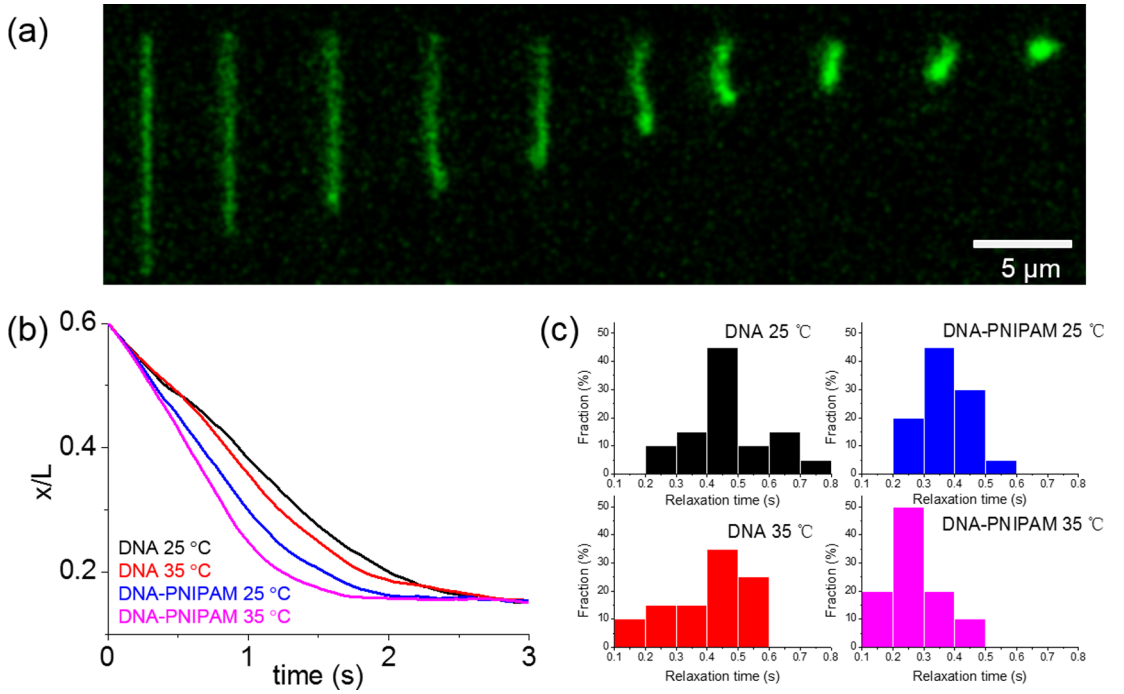

Figure 4. Longest relaxation time of surface-tethered DNA-PNIPAM and DNA polymers as a function of temperature. (a) Time-lapse images showing relaxation of a single DNA-PNIPAM copolymer (30 kbp DNA backbone) at 25 °C after the cessation of shear flow. Time between snapshots is 0.25 s. (b) Ensemble-averaged relaxation trajectories of single DNA-PNIPAM copolymers and DNA polymers (minimum of N = 20 molecules in each ensemble). (c) Longest relaxation time distribution of single DNA-PNIPAM copolymers and DNA polymers (30 kbp DNA backbone, minimum of N = 20 molecules in each ensemble).

temperature transitions. These results suggest that PNIPAM side branches transition from hydrophilic to hydrophobic when the temperature is raised above the LCST, thereby resulting in chain collapse of the DNA-PNIPAM copolymers at 40 °C.

DOI: 10.1021/acsmacrolett.8b00016
ACS Macro Lett. 2018, 7, 281−286

In a second set of experiments, we studied the effect of branch density on the DNA-PNIPAM copolymer length distribution (Figure 3d, Figure S3, and Table S3). For these experiments, the stretched length distributions of 10 kbp DNA-PNIPAM samples (13 kDa PNIPAM) with low branch loadings (1% DBCO-dUTP) and high branch loadings (10% DBCO-dUTP) were determined in shear flow at 25 and 40 °C. In general, our results show that samples with higher branch densities exhibit larger degrees of intramolecular collapse to shorter size upon increasing temperature to 40 °C. These results are consistent with the notion that higher levels of PNIPAM side branches induce stronger degrees of intramolecular hydrophobicity when the temperature is raised above the LCST. We further studied the effect of PNIPAM branch molecular weight on stretched length distribution of DNA copolymers in flow (Figure 3e, Figure S4, and Table S3). For these experiments, we focused on DNA-PNIPAM with 1% substitution containing PNIPAM side branches with a molecular weight of 13 kDa or 30 kDa. Single-molecule experiments show that stretched length distributions for DNA-PNIPAM copolymers are shifted to slightly smaller sizes using increasing PNIPAM molecular weight, which is again consistent with the hypothesis that larger PNIPAM sizes result in stronger intramolecular hydrophobicity interactions for temperatures above the LCST.

We next used single-molecule fluorescence microscopy to study the conformational relaxation dynamics of surface-tethered thermoresponsive DNA copolymers (Figure 4). In this experiment, surface-immobilized polymers were first stretched to high degrees of extension in flow, followed by abrupt cessation of fluid flow. Single polymer chains are then allowed to relax back to a thermally equilibrated state, and the relaxation trajectories of single chains are observed. In this experiment, we determined the effect of temperature on the conformational relaxation dynamics of DNA-PNIPAM copolymers. Here, we focus on DNA-PNIPAM with 30 kbp DNA backbones with 1% substitution with 13 kDa PNIPAM. Polymer relaxation is studied above and below the LCST (25 and 35 °C, respectively). Interestingly, we found that >70% of DNA-PNIPAM polymers (30 kbp DNA with 13 kDa PNIPAM branches) stretch to >80% of the theoretical contour length at 35 °C, which allows for direct measurement of polymer relaxation trajectories. However, chain extension is greatly inhibited at 40 °C, such that only <10% of polymer chains stretch to 80% of the theoretical contour length in tethered shear flow at 40 °C. For these reasons, we performed polymer relaxation experiments at 35 °C, which allows for quantification of polymer relaxation over a large ensemble of molecules.

A series of time-lapse images of a single DNA-PNIPAM copolymer relaxing from high extension are shown in Figure 4a. Transient single polymer relaxation data are analyzed to determine fractional extension of the polymer backbone (x/L) by normalizing the dimensional chain extension x with the backbone contour length ($L \approx 13.6$ μm for 30 kbp DNA). This experiment is performed over a large molecular ensemble ($N > 20$), thereby enabling determination of the longest relaxation time of each sample by fitting average relaxation data over the regime $0.14 < x/L < 0.30$ to a Rouse-inspired single exponential decay: $(x/L)^2 = a \exp(-t/\tau) + b$, where t is time, τ is the longest relaxation time of the polymer, and a and b are fitting constants.[36,37] In this way, we determine the longest relaxation time for DNA ($\tau_{\text{DNA,25 °C}} = 0.45 \pm 0.11$ s, $\tau_{\text{DNA,35 °C}} = 0.42 \pm 0.14$ s) and DNA-PNIPAM ($\tau_{\text{DNA-PNIPAM,25 °C}} = 0.36 \pm 0.08$ s, $\tau_{\text{DNA-PNIPAM,35 °C}} = 0.27 \pm 0.09$ s), respectively (Figure 4b and Figure 4c). However, we note that these experiments are performed in an aqueous buffer (10 mM Tris/Tris-HCl, pH 8.0, 1 mM EDTA, and 5 mM NaCl) that exhibits a temperature-dependent viscosity. In order to isolate the effects of changes in longest polymer relaxation time due to hydrophilic/hydrophobic interactions of PNIPAM, we rescale the longest relaxation times with solvent viscosity at a given temperature. In this way, we determine a normalized longest relaxation time for DNA and DNA-PNIPAM that arises due to PNIPAM hydrophobic interactions. In particular, we find $\tau_{\text{DNA,25 °C}} = 0.32 \pm 0.08$ s/cP, $\tau_{\text{DNA,35 °C}} = 0.33 \pm 0.11$ s/cP for natural DNA, $\tau_{\text{DNA-PNIPAM,25 °C}} = 0.26 \pm 0.06$ s/cP, and $\tau_{\text{DNA-PNIPAM,35 °C}} = 0.21 \pm 0.07$ s/cP for DNA-PNIPAM copolymers, respectively. These results show that the PNIPAM side branches have a direct impact on polymer relaxation. DNA-PNIPAM copolymers relax faster due to PNIPAM intramolecular interactions compared to natural DNA without PNIPAM side branches above the LCST.

In this letter, we report the direct observation of DNA-PNIPAM copolymer dynamics using single-molecule techniques. Thermoresponsive DNA-PNIPAM copolymers are synthesized via copper-free click chemistry, and single-molecule imaging is used to study the effect of PNIPAM branches the stretched the length distribution of surface-tethered polymers in shear flow and the conformational relaxation dynamics following cessation of flow. From a broad perspective, our results show that DNA-PNIPAM copolymers show a broad degree of dynamic heterogeneity in relaxation and steady stretching dynamics due to the presence of PNIPAM side branches, in particular above the LCST. We observe that higher branch densities and higher branch molecular weights tend to induce polymer collapse for temperatures above the LCST. To our knowledge, this work is one of the first studies to extend single-molecule imaging to DNA copolymers, with a particular emphasis on heterogeneous chain dynamics. Future work aimed at direct observation of hierarchical assembly of DNA-based copolymers and transient stretching dynamics for chemically and/or topologically complex polymeric materials such as stimuli-responsive systems holds the potential to provide new molecular insights into dynamic supramolecular assembly processes and could lead to new molecular designs to serve as drug and gene delivery carriers.

■ ASSOCIATED CONTENT

Supporting Information

The Supporting Information is available free of charge on the ACS Publications website at DOI: 10.1021/acsmacrolett.8b00016.

Details of DNA-PNIPAM polymer synthesis, microdevice fabrication, surface preparation, and single-molecule imaging (PDF)

■ AUTHOR INFORMATION

Corresponding Author

*E-mail: cms@illinois.edu.

ORCID

Charles M. Schroeder: 0000-0001-6023-2274

Notes

The authors declare no competing financial interest.

DOI: 10.1021/acsmacrolett.8b00016
ACS Macro Lett. 2018, 7, 281−286

■ ACKNOWLEDGMENTS

This work was funded by an NSF CAREER Award CBET-1254340 and the Camille and Henry Dreyfus Foundation for CMS. The authors acknowledge the Frederick Seitz Materials Research Laboratory for electron microscopy and imaging facilities. We thank Y. Bai, H. Ying, J. Turner, and J. Serrano for their technical help.

■ REFERENCES

(1) Aida, T.; Meijer, E. W.; Stupp, S. I. Functional Supramolecular Polymers. *Science* **2012**, *335* (6070), 813−817.
(2) Qiu, H.; Hudson, Z. M.; Winnik, M. A.; Manners, I. Multidimensional Hierarchical Self-Assembly of Amphiphilic Cylindrical Block Comicelles. *Science* **2015**, *347* (6228), 1329−1332.
(3) Lutz, J.-F.; Lehn, J.-M.; Meijer, E. W.; Matyjaszewski, K. From Precision Polymers to Complex Materials and Systems. *Nature Reviews Materials* **2016**, *1* (5), 16024.
(4) Frechet, J. Functional Polymers and Dendrimers: Reactivity, Molecular Architecture, and Interfacial Energy. *Science* **1994**, *263* (5154), 1710−1715.
(5) Yin, Q.; Tang, L.; Cai, K.; Tong, R.; Sternberg, R.; Yang, X.; Dobrucki, L. W.; Borst, L. B.; Kamstock, D.; Song, Z.; Helferich, W. G.; Cheng, J.; Fan, T. M. Pamidronate Functionalized Nanoconjugates for Targeted Therapy of Focal Skeletal Malignant Osteolysis. *Proc. Natl. Acad. Sci. U. S. A.* **2016**, *113* (32), E4601−9.
(6) Yuan, Y.; Zhang, C. J.; Liu, B. A Photoactivatable Aie Polymer for Light-Controlled Gene Delivery: Concurrent Endo/Lysosomal Escape and DNA Unpacking. *Angew. Chem., Int. Ed.* **2015**, *54* (39), 11419−23.
(7) McHale, R.; Patterson, J. P.; Zetterlund, P. B.; O'Reilly, R. K. Biomimetic Radical Polymerization Via Cooperative Assembly of Segregating Templates. *Nat. Chem.* **2012**, *4* (6), 491−497.
(8) Wang, Z.; van Oers, M. C.; Rutjes, F. P.; van Hest, J. C. Polymersome Colloidosomes for Enzyme Catalysis in a Biphasic System. *Angew. Chem., Int. Ed.* **2012**, *51* (43), 10746−50.
(9) Yu, Z.; Tantakitti, F.; Yu, T.; Palmer, L. C.; Schatz, G. C.; Stupp, S. I. Simultaneous Covalent and Noncovalent Hybrid Polymerizations. *Science* **2016**, *351* (6272), 497−502.
(10) Li, B.; Li, S.; Zhou, Y.; Ardona, H. A.; Valverde, L. R.; Wilson, W. L.; Tovar, J. D.; Schroeder, C. M. Nonequilibrium Self-Assembly of Pi-Conjugated Oligopeptides in Solution. *ACS Appl. Mater. Interfaces* **2017**, *9* (4), 3977−3984.
(11) Mirkin, C. A.; Letsinger, R. L.; Mucic, R. C.; Storhoff, J. J. A DNA-Based Method for Rationally Assembling Nanoparticles into Macroscopic Materials. *Nature* **1996**, *382* (6592), 607−609.
(12) Marciel, A. B.; Mai, D. J.; Schroeder, C. M. Template-Directed Synthesis of Structurally Defined Branched Polymers. *Macromolecules* **2015**, *48* (5), 1296−1303.
(13) Schnitzler, T.; Herrmann, A. DNA Block Copolymers: Functional Materials for Nanoscience and Biomedicine. *Acc. Chem. Res.* **2012**, *45* (9), 1419−1430.
(14) Wilks, T. R.; Bath, J.; de Vries, J. W.; Raymond, J. E.; Herrmann, A.; Turberfield, A. J.; O'Reilly, R. K. Giant Surfactants" Created by the Fast and Efficient Functionalization of a DNA Tetrahedron with a Temperature-Responsive Polymer. *ACS Nano* **2013**, *7* (10), 8561−8572.
(15) Peterson, A. M.; Heemstra, J. M. Controlling Self-Assembly of DNA-Polymer Conjugates for Applications in Imaging and Drug Delivery. *Wiley interdisciplinary reviews. Nanomedicine and nanobiotechnology* **2015**, *7* (3), 282−97.
(16) Kim, C. J.; Hu, X.; Park, S. J. Multimodal Shape Transformation of Dual-Responsive DNA Block Copolymers. *J. Am. Chem. Soc.* **2016**, *138* (45), 14941−14947.
(17) Ding, K.; Alemdaroglu, F. E.; Borsch, M.; Berger, R.; Herrmann, A. Engineering the Structural Properties of DNA Block Copolymer Micelles by Molecular Recognition. *Angew. Chem., Int. Ed.* **2007**, *46* (7), 1172−5.
(18) Albert, S. K.; Thelu, H. V.; Golla, M.; Krishnan, N.; Chaudhary, S.; Varghese, R. Self-Assembly of DNA-Oligo(P-Phenylene-Ethynylene) Hybrid Amphiphiles into Surface-Engineered Vesicles with Enhanced Emission. *Angew. Chem., Int. Ed.* **2014**, *53* (32), 8352−7.
(19) Vyborna, Y.; Vybornyi, M.; Rudnev, A. V.; Haner, R. DNA-Grafted Supramolecular Polymers: Helical Ribbon Structures Formed by Self-Assembly of Pyrene-DNA Chimeric Oligomers. *Angew. Chem., Int. Ed.* **2015**, *54* (27), 7934−8.
(20) Shaqfeh, E. S. G. The Dynamics of Single-Molecule DNA in Flow. *J. Non-Newtonian Fluid Mech.* **2005**, *130* (1), 1−28.
(21) Mai, D. J.; Schroeder, C. M. Single Polymer Dynamics of Topologically Complex DNA. *Curr. Opin. Colloid Interface Sci.* **2016**, *26*, 28−40.
(22) Schroeder, C. M. Single Polymer Dynamics for Molecular Rheology. *J. Rheol.* **2018**, *62* (1), 371−403.
(23) Perkins, T. T.; Smith, D. E.; Chu, S. Single Polymer Dynamics in an Elongational Flow. *Science* **1997**, *276* (5321), 2016−2021.
(24) Schroeder, C. M.; Babcock, H. P.; Shaqfeh, E. S.; Chu, S. Observation of Polymer Conformation Hysteresis in Extensional Flow. *Science* **2003**, *301* (5639), 1515−1519.
(25) Li, Y.; Hsiao, K.-W.; Brockman, C. A.; Yates, D. Y.; Robertson-Anderson, R. M.; Kornfield, J. A.; San Francisco, M. J.; Schroeder, C. M.; McKenna, G. B. When Ends Meet: Circular DNCA Stretches Differently in Elongational Flows. *Macromolecules* **2015**, *48* (16), 5997−6001.
(26) Mai, D. J.; Marciel, A. B.; Sing, C. E.; Schroeder, C. M. Topology-Controlled Relaxation Dynamics of Single Branched Polymers. *ACS Macro Lett.* **2015**, *4* (4), 446−452.
(27) Marciel, A. B.; Schroeder, C. M. New Directions in Single Polymer Dynamics. *J. Polym. Sci., Part B: Polym. Phys.* **2013**, *51* (7), 556−566.
(28) Zhou, Y.; Schroeder, C. M. Single Polymer Dynamics under Large Amplitude Oscillatory Extension. *Physical Review Fluids* **2016**, *1* (5), 053301.
(29) Hsiao, K.-W.; Sasmal, C.; Ravi Prakash, J.; Schroeder, C. M. Direct Observation of DNA Dynamics in Semidilute Solutions in Extensional Flow. *J. Rheol.* **2017**, *61* (1), 151−167.
(30) Schild, H. G. Poly(N-Isopropylacrylamide): Experiment, Theory and Application. *Prog. Polym. Sci.* **1992**, *17* (2), 163−249.
(31) Okada, Y.; Tanaka, F. Cooperative Hydration, Chain Collapse, and Flat Lcst Behavior in Aqueous Poly(N-Isopropylacrylamide) Solutions. *Macromolecules* **2005**, *38* (10), 4465−4471.
(32) Saha, S.; Heuer, D. M.; Archer, L. A. Electrophoretic Mobility of Linear and Star-Branched DNA in Semidilute Polymer Solutions. *Electrophoresis* **2006**, *27* (16), 3181−3194.
(33) Pan, S.; Nguyen, D. A.; Sridhar, T.; Sunthar, P.; Prakash, J. R. Universal Solvent Quality Crossover of the Zero Shear Rate Viscosity of Semidilute DNA Solutions. *J. Rheol.* **2014**, *58* (2), 339−368.
(34) Selvin, P. R.; Ha, T. *Single-Molecule Techniques*; Cold Spring Harbor Laboratory Press: 2008.
(35) Ladoux, B.; Doyle, P. S. Stretching Tethered DNA Chains in Shear Flow. *EPL (Europhysics Letters)* **2000**, *52* (5), 511.
(36) Doi, M.; Edwards, S. F. *The Theory of Polymer Dynamics*; Oxford University Press: 1988; Vol. *73*.
(37) Rouse, P. E. A Theory of the Linear Viscoelastic Properties of Dilute Solutions of Coiling Polymers. *J. Chem. Phys.* **1953**, *21* (7), 1272−1280.

DOI: 10.1021/acsmacrolett.8b00016
ACS Macro Lett. 2018, 7, 281−286